**Squaraine dyes as fluorescent turn-on sensors for the detection of porcine gastric mucin: A spectroscopic and kinetic study**

# Squaraine dyes as fluorescent turn-on sensors for the detection of Porcine Gastric Mucin: a spectroscopic and kinetic study

Cosmin Butnarasu, [a] Nadia Barbero, [b] Claudia Barolo, [b] and Sonja Visentin[a]

[a] Department of Molecular Biotechnology and Health Sciences, University of Torino, Via Gioacchino Quarello 15A, 10135 Torino (Italy)

[b] Department of Chemistry, NIS Interdepartmental and INSTM Reference Centre, University of Torino, Via Pietro Giuria 7, 10125 Torino (Italy)

**Abstract**

Mucins glycoproteins are the principal components of mucus which cover all the mucosal surfaces of the human body. The mucus and mucins are essential mediators of the innate immune system, however in the last decades mucins have been identified even as an important class of cancer biomarkers. Luminogenic materials with fluorescence turn-on behavior are becoming promising materials because of their advantages of label free, relatively inexpensive and simple to use properties for biological detection and imaging. Squaraines are luminogens characterized by high fluorescence in organic media but poor emission in aqueous environments due to their tendency to self-aggregate. Herein we investigate the interaction between porcine gastric mucin (PGM) and several squaraines in aqueous media. While squaraine dyes showed low fluorescence intensity and quantum yield in water, as a result of the formation of aggregates, an enhancement of fluorescence up to 45-fold was achieved when PGM was added. PGM was detected in a linear range of 10-300 µg/mL with a limit of detection of 800 ng/mL. The assay was used to quantify mucin in diluted human serum samples and recoveries of 94.9-116.2% were achieved. To the best of our knowledge, this is the easiest and convenient method for mucin detection in the reported literature.

***Keywords.*** Squaraines, turn-on, UV-Vis, fluorescence, porcine gastric mucin, kinetics

## 1. Introduction

Mucins are a family of long polymeric glycoconjugates having high molecular weight, produced by goblet cells in the gastrointestinal, respiratory, reproductive, pancreatic, hepatic and renal epithelium. Structurally, mucins are formed by a long peptide core at which glycans are linked (Figure 1 A). So far, two major classes of mucins have

been identified: secreted mucins, further divided as gel-forming and non-gel forming, and transmembrane mucins[1–3]. Gel-forming mucins assemble into polymers creating a complex network representing the skeleton around which mucus is formed [4]. The primary function of mucus is to protect the underlying surfaces from environmental stressors. Beside its protective function, in pathological conditions, mucus can become a concentrate of pathogens and cellular debris as well as a barrier for drug absorption as a result of its altered physico-chemical properties. Alterations or overexpression of mucus are associated with diseases like chronic obstructive pulmonary disease (COPD), asthma, cystic fibrosis and several types of cancer [5]. Particularly, in the last years, great attention was addressed to expression of mucins in various cancers such as pancreatic adenocarcinomas [6,7], colon and rectal cancer [8], breast cancer [9], ovarian cancer [10] and gastric carcinoma [11]. Maker *et al.* [12] found that high-risk patients for intraductal papillary mucinous neoplasms of the pancreas have elevated cyst fluid concentrations of MUC2 and MUC4, and increased serum levels of MUC5AC. Significantly high serum levels of MUC2 were found also in patients with breast cancer. It is well known that the early diagnosis is a key factor for outcome, treatments, and healthcare. Thus, the identification and detection of specific and sensitive biomarkers have become extremely important in the last decades [12–16].

Up until now, various methods for membrane-bound mucin MUC1 detection have been developed such as antibody-based enzyme-linked immunosorbent assays and aptamer-based electrochemical and fluorescence techniques [17–20]. However, these methods often have limitations including relative instability, complex production, difficult purification processes, and time-consuming. Therefore, the search for better alternatives is still running. Among the above mentioned methods, fluorometric assays have received remarkable attention due to their convenience, unparalleled sensitivity, simplicity, rapid implementation, noninvasive monitoring capability and usability in biological samples [21]. Thus, the interest in developing new dyes that can non-covalently bind specific proteins for their detection is rising up. Fluorescent probes with absorption and emission in the near infrared (NIR) region (650-900 nm) are useful for practical biological applications as NIR signal detection does not suffer of self-absorption and autofluorescence typical of biological matrices.

Among promising biological fluorescent probes, polymethine dyes (cyanine and squaraines) are characterized by sharp and intense absorption and emission in the visible up to the NIR region. Squaraine dyes are produced by condensation reactions between squaric acid and electron-rich substrates. Squaraines were studied extensively and such research covered numerous areas ranging from photophysical to biological applications [22–24]. Moreover, we can easily design and modify their structure to get NIR molecules, perfectly matching the phototherapeutic window (650-850 nm), simply by tuning the lateral functional groups [25,26]. However, as most of fluorescent probes, in physiological conditions, squaraine dyes tend to form aggregates that lead to fluorescence quenching therefore limiting their wide applications. As reported in previous studies, squaraine dyes exhibit a fluorescence turn-on when bound to proteins which translate in an increase in fluorescence intensity, quantum yield and lifetime due to the changes in the surrounding environment [27–31].

In the present paper we report our results about a spectroscopic, thermodynamic and kinetic study of the interaction between commercial porcine gastric mucin (PGM) and four squaraine dyes with different substitutions (Figure 1 B). The squaraines differ on the nature of the lateral moieties (i.e. indolenine vs benzoindolenine) and on the length of the alkyl chains (i.e. C2 vs C8). Interactions were carried out by means of UV-Vis, circular dichroism and fluorescence spectroscopies. Moreover, we evaluate the possibility of using these squaraine dyes as probes for mucin detection in serum samples. We report a new fluorometric “turn-on” detection of mucin based on the aggregation/deaggregation of squaraine dyes in different environments. As far as we know, no reports have been published to date on the application of squaraine dyes as fluorescent probes in testing mucin detection in human serum samples.

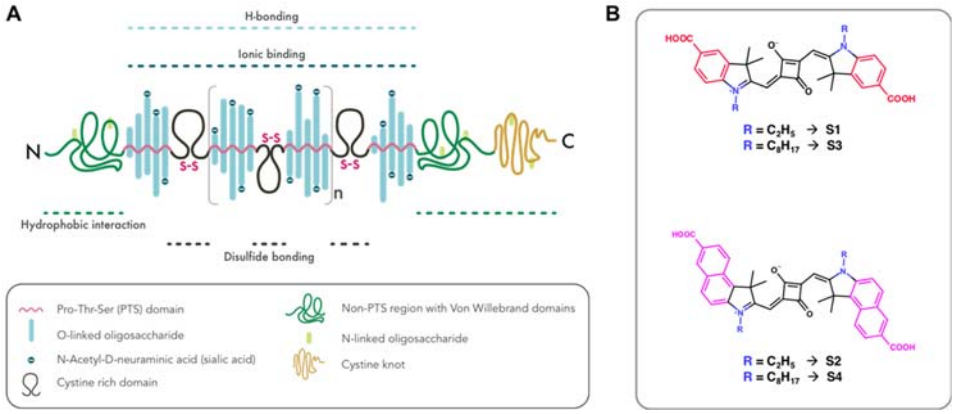


**Figure 1**. Molecular structures of PGM (A, adapted from Butnarasu *et al.* [32]) and the squaraine dyes (B).

## 2. Experimental section

### 2.1. Materials

All reagents were of analytical reagent grade. Millipore grade water was obtained from an in-house Millipore system (resistivity: 18.2 MΩ cm at 25 °C). Mucin from porcine stomach (PGM type III, bound sialic acid 0.5-1.5%, partially purified powder) was purchased from Sigma Aldrich. PGM solutions were prepared in water. Since PGM itself is a water insoluble material, in order to facilitate solubility in water and obtain homogeneous suspensions, dispersions of mucin were sonicated for two minutes at room temperature. Squaraine dyes were prepared as previously described [33]. Mother solutions of the dyes (500 µg/mL) were prepared in DMSO and dilutions for the experiments (in the µM range) were performed in water.

### 2.2. Spectroscopic measurements

UV-Vis absorption spectra were measured by a UH5300 Hitachi spectrophotometer at room temperature, using 1 cm pathway length quartz cuvettes. The UV measurements were made in the range of 500-750 nm. Squaraine dyes concentration was kept constant (2 µM) and PGM changed over the range 0-300 µg/mL.

Circular dichroism measurements were performed using a Jasco J-815 CD spectrophotometer. The spectra were collected in a range of 185-250 nm in a quartz cuvette with a 0.5 mm light path using a scan speed of 50 nm/min. Each spectrum is the average of three scans.

Fluorescence emission spectra in steady state mode were acquired at room temperature using a Horiba Jobin Yvon Fluorolog 3 TCSPC fluorimeter equipped with a 450-W Xenon lamp and a Hamamatsu R928 photomultiplier.

Fluorescence spectra were recorded in the range of 615-750 nm for S1, 625-800 nm for S3 and 645-800 nm for S2 and S4. The excitation wavelength was fixed on the squaraine hypsochromic shoulder of absorbance: 595 nm for S1, 605 nm for S3 and 625 nm for S2 and S4. A constant concentration of squaraine dye (1 µM for S1 and S2, and 0.1 µM for S3 and S4) was analysed by successive increasing the concentration of PGM.

Fluorescence experiments were also performed in a time drive mode in order to check whether and when the solution reached the stability; fluorescence intensity of a constant concentration of squaraine and PGM was registered over time at specific time points.

The absolute quantum yield was determined by means of an integrating sphere combining Quanta-φ with Fluorolog 3. The reported quantum yields are the average of the values obtained after three measurements using three different dye solutions.

Fluorescence lifetimes were measured by the time correlated single photon counting method (Horiba Jobin Yvon) using a 636 nm Horiba Jobin Yvon NanoLED as excitation source and an impulse repetition frequency of 1 MHz positioned at 90° with respect to a TBX-04 detector. Lifetimes were calculated using DAS6 decay analysis software.

### 2.3 Serum test

To assess applicability for detecting PGM in complex matrices, we performed measurements in diluted human serum (HS). Serum samples were prepared as following. To a volume of HS, an equal volume of cold 50% w/v trichloroacetic acid (TCA) was added. The sample was vortexed for one minute and then stored at -20 °C for 15 min. Next, the sample was centrifuged at 13.000 rpm for 15 min at 4 °C. The supernatant was collected and centrifuged again using the same settings. Eventually, the supernatant was collected, neutralized with NaOH 1 M and 1% diluted HS samples were prepared in water. Spiked samples were prepared by addition of different concentrations of PGM to the diluted HS.

## 3. Results and Discussion

### 3.1. Spectroscopic measurements

The absorption and emission of squaraine dyes are strongly influenced by the environment [29]. First the UV/Vis absorption spectra of the four squaraines were recorded in different solvents (Figure 2). All the four squaraines are freely soluble in DMSO giving one principal band at 656, 684, 659 and 686 nm attributing it to the monomeric form of S1, S2, S3 and S4 respectively, and a slight shoulder at lower wavelengths. The absorption spectra of the four squaraines in water are blue-shifted with a decreased absorbance that is a consequence of the reduced solubility. This is particularly evident for S3 and S4 where the monomeric band is almost absent, and the absorption spectrum is characterized by the large H-aggregate band. Except for S1, the addition of surfactants (SDS or Pluronic F-127, 0.05 wt %) to the aqueous solution leads to an increase in absorption of the band corresponding to the monomeric form. The major changes in absorption are achieved with the non-ionic surfactant (Pluronic F-127). Since the concentration of surfactants are below their critical micelle concentration (CMC), the surfactant molecules are expected to be not aggregated. As proposed by Y. Xu et al. [28] it is possible that the negative charge of SDS interacts with the positively charged (even if delocalized) nitrogen of the squaraines, making them more soluble in water thus less aggregated. Likewise, the hydrophobic poly(propylene)-oxide (PPO) segments of the amphiphilic surfactant (Pluronic F-127) may entangle with the indolenine or benzoindolenine moieties of the squaraine resulting in an increased water solubility. An increase in solubility, even if particularly evident only for S3, is achieved with phosphate buffer (2 mM, pH 7.4). At pH 7.4 the carboxylic groups on the lateral moieties of squaraines are completely deprotonated consequently resulting in an increased solubility in water.

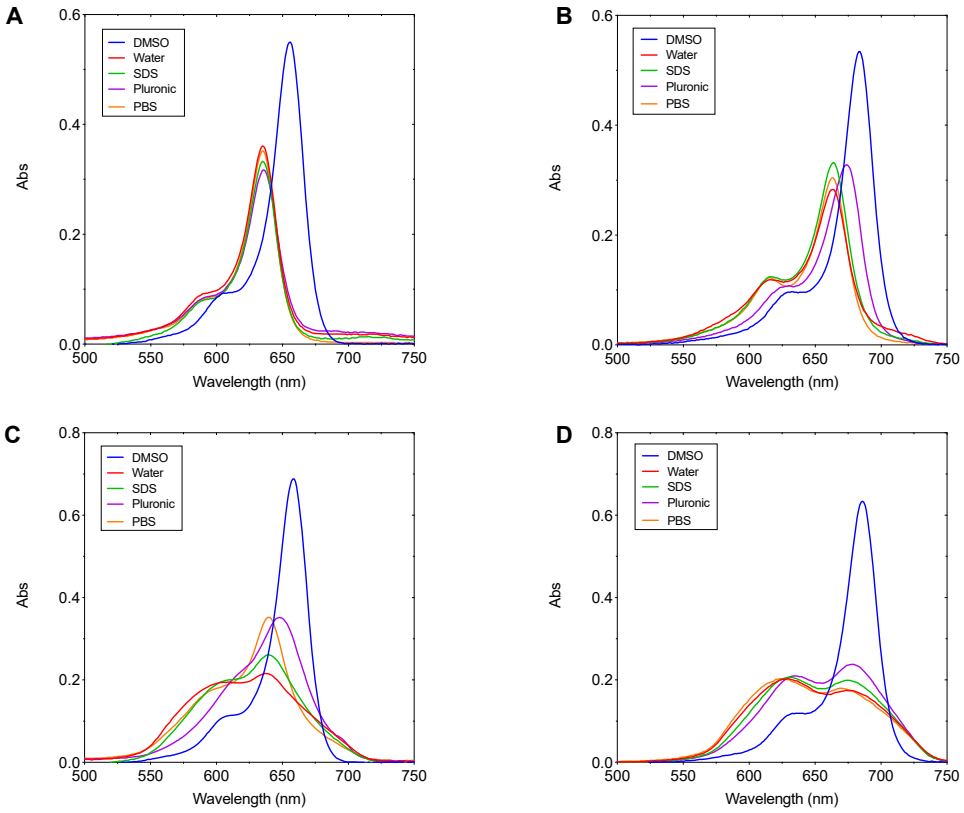


**Figure 2.** UV/Vis absorption spectra of a 2 μM solution of S1 (A), S2 (B), S3 (C), S4 (D) recorded in different solvents.

The interaction between each squaraine and PGM was firstly monitored by UV/Vis absorption spectroscopy keeping the squaraine concentration constant (1 μM) with a subsequent increase amount of PGM (Figure 3). Since mucin "solutions" are actually suspensions, with the increasing of the concentration of the protein we observe an increase of the absorption baseline which is the result of the suspended mucin strands. Addition of increasing amounts of PGM to the solutions of the short-chain squaraines, S1 and S2, results in an increased absorption (hyperchromism) of their bands at 636 and 663 nm respectively. The absorption spectra of the two squaraines with the longer chains, S3 and S4, are characterized by two large bands; the first band at shorter wavelength assignable to H-aggregates, while the second one at longer wavelength accountable to the monomeric form of the squaraine. In the case of S3, addition of PGM resulted in a gradually increase of the band at 639 nm and a decrease of the H-aggregate band at 612 nm. A similar trend was observed also for S4. Here, not only the bands at 627 and 673 nm decreased and increased but were also 4 and 10 nm red-shifted respectively. Overall, these results suggest that in presence of PGM a lower amount of H-aggregates is present and probably the protein interacts with the monomeric form of the squaraine dye. However, the exact mechanism of interaction is not fully understood with only this technique.

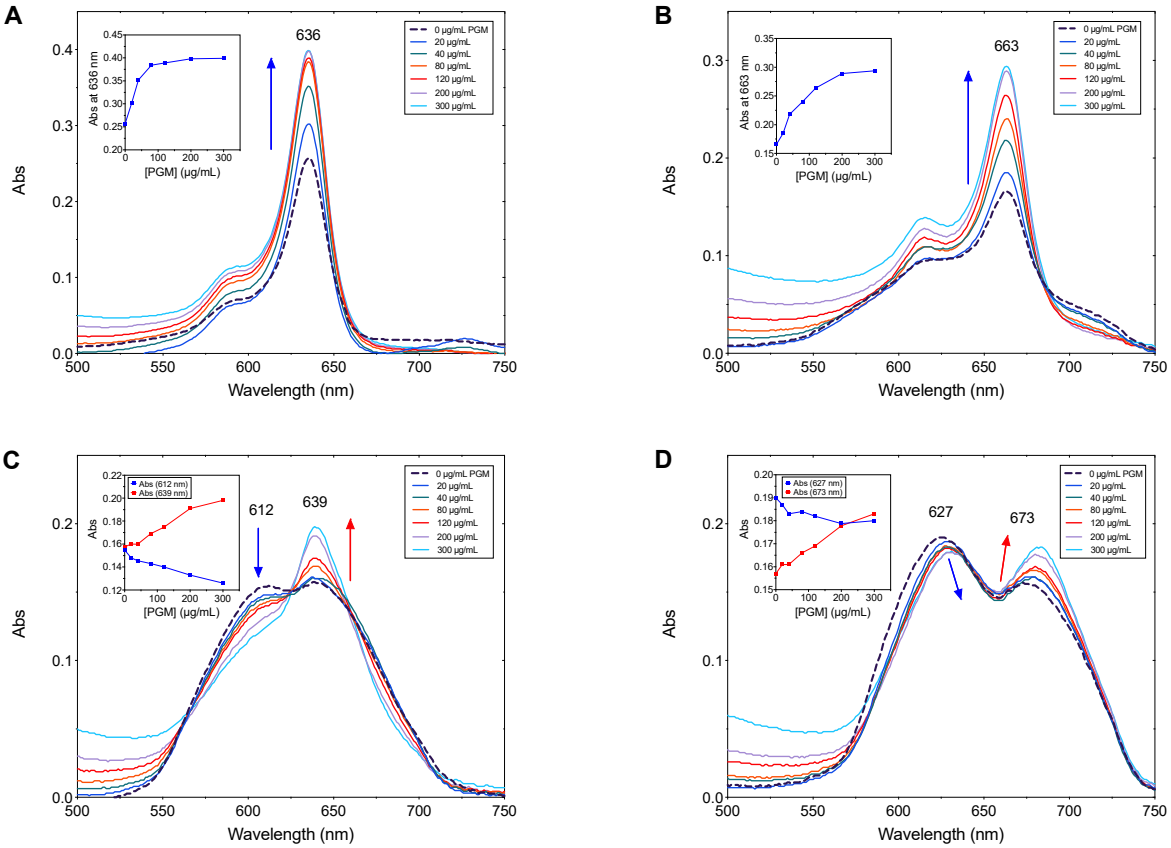


**Figure 3**. UV/Vis absorption spectra of S1 (A), S2 (B), S3 (C) and S4 (D) alone (bold dashed line) and upon addition of porcine gastric mucin (PGM). The inset shows the absorbance response to PGM concentration.

As reported also in our previous studies, all the herein studied squaraines have excellent emission properties in organic solvents which is gradually decreased, due to an aggregation quenching effect (AQE), upon addition of increasingly amount of water [22,27,34]. The loss of fluorescent features of squaraines as a result of the aggregation phenomenon is widely reported in literature [29,35–39]. When the concentration of PGM was increased in the test system, a gradual enhancement in the fluorescence intensity was observed (Figure 4). In fact, the emission intensity of S1 at about 642 nm increased about 3 times, while for S2 the fluorescence intensity increased about 4 times and the original emission peak at 670 nm was 7 nm red-shifted. Interestingly, the major turn-on of fluorescence was recorded for the complexes with the analogue squaraine dyes with longer alkyl chains (S3 and S4). Indeed, upon addition of PGM, the maximum emission wavelength of S3 shifted from 645 to 660 nm and the fluorescence intensity increased by almost 45-fold. Similarly, a red-shift from 676 to 687 nm with a 40-fold emission enhancement was observed for the S4/PGM complex. The PGM-induced increase of fluorescence is visible even by naked eye when the beam of the spectrofluorometer is passing the quartz cuvette (insets on Figure 4).

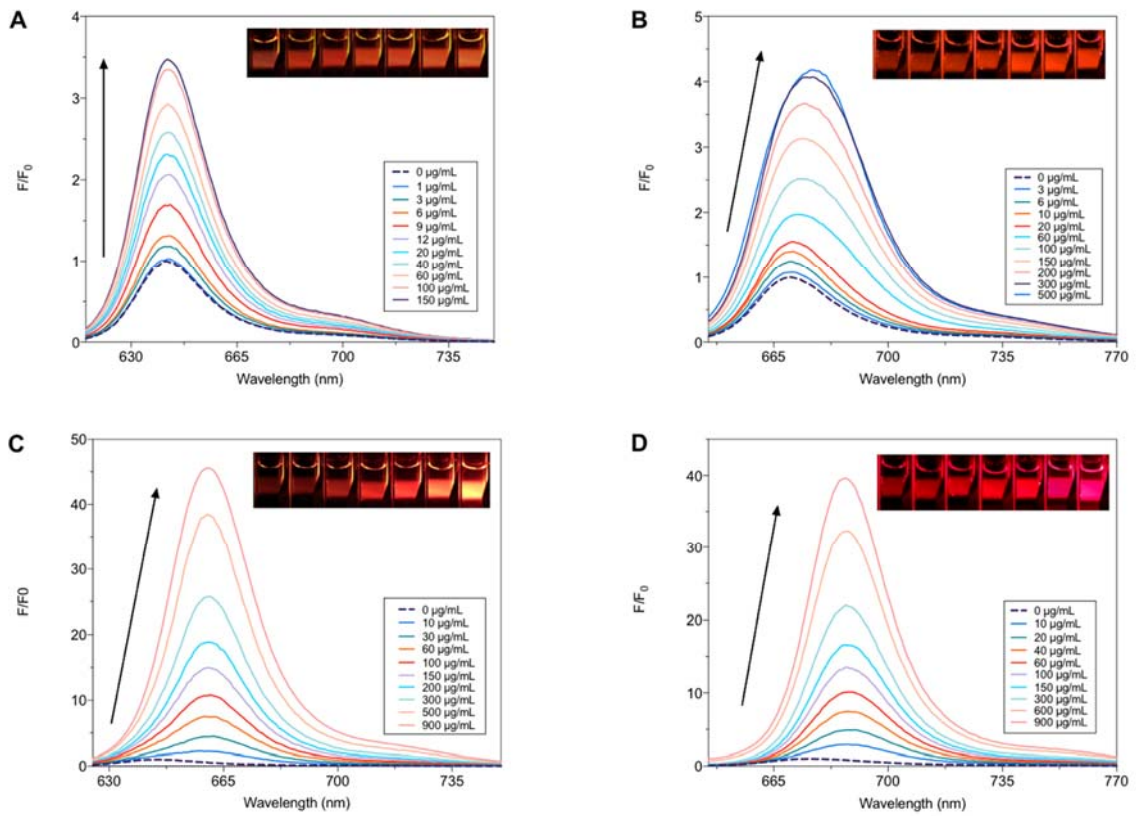


**Figure 4**. Steady-state fluorescence intensity changes of S1 (A), S2 (B), S3 (C) and S4 (D) upon addition of PGM. The inset show the increase of emission visible on the surface of cuvette.

The observed increase of fluorescence and the red-shift after the introduction of PGM indicated environmental changes surrounding the squaraine chromophore. Squaraine aggregates may entangle with the hydrophobic domains of mucin. Once the contact is established, single dye molecules could be released from the aggregate to freely interact with the protein (inset in Figure 10). As mentioned above, the emission spectra of the monomeric form of the squaraines can be registered in organic solvents like DMSO. In Figure 5 it can be seen that, except for S1, the emission profile of squaraines recorded in aqueous solutions of mucin are shifted toward the profile of squaraines registered in DMSO. Moreover, it is noteworthy to mention that the emission intensity of S3-PGM complex is almost intense (>80%) as the emission of S3 alone recorded in DMSO. These observations suggest that the emission turn-on may be attributed to an increase in the hydrophobicity of the environment surrounding the squaraine due to the hydrophobic domains of mucin. To test if the dye-protein interaction is somehow dependent by the hydrophobic domains of mucin we recorded the emission of squaraines in presence of PGM at pH 2. It is known that at acidic pH, the hydrophobic domains of mucin are involved in non-covalent crosslinks via hydrophobic associations [3,40]. As can be seen in Figure 5, at acidic pH the emission intensity of the squaraines in presence of mucin is reduced. These results indicate that the acidic-induced modification of the structure of mucin makes less effective the contact with squaraine aggregates, so giving a reduced turn-on of fluorescence.

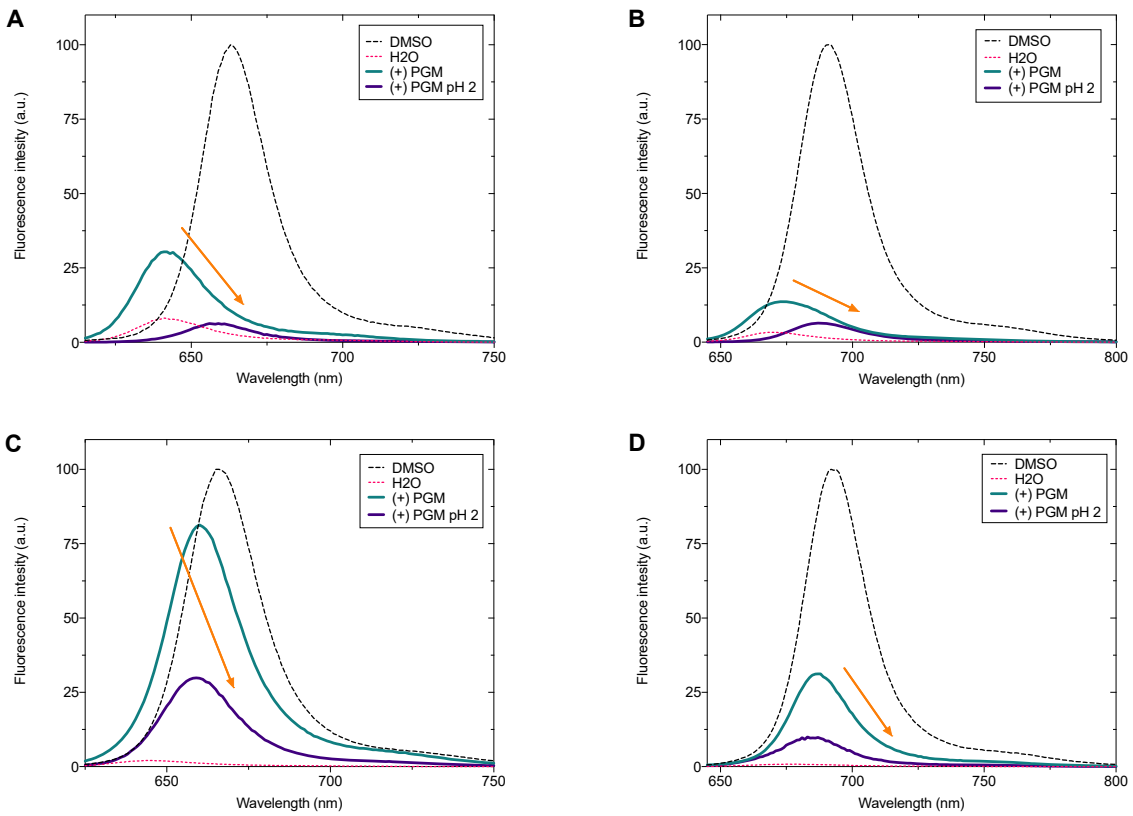


**Figure 5**. Steady-state fluorescence intensity of S1 (A), S2 (B), S3 (C) and S4 (D) registered in DMSO, in water, in aqueous solutions of PGM and in aqueous solutions of PGM adjusted at pH 2.

To further confirm the hypothesis that the nature of the binding forces involved in the interaction of squaraines with PGM are of hydrophobic nature, we performed a thermodynamic study. Squaraines with the major ratio of $F/F_0$ (i.e. S3 and S4) were analyzed. A constant concentration of squaraine was titrated with mucin at different temperatures (288, 296, 310 K) and the fluorescence spectra were recorded. According to the values of enthalpy and entropy changes, the model of interaction between two chemical species can be summarized as: (i) $\Delta H°>0$ and $\Delta S°>0$ are indicative of binding guided by hydrophobic forces; (ii) $\Delta H°<0$ and $\Delta S°<0$ interactions through van der Waals interactions and hydrogen bonds; (iii) $\Delta H°<0$ and $\Delta S°>0$ are indicative of electrostatic interactions [32]. The various thermodynamic parameters, enthalpy change ($\Delta H°$), entropy change ($\Delta S°$) and Gibbs free energy change ($\Delta G°$) were calculated using the van't Hoff equation (*Eq.* 1 and *Eq.* 2) as mentioned below:

$$lnK = -\frac{\Delta H°}{RT} + \frac{\Delta S°}{R} \qquad (Eq.1)$$

$$\Delta G° = \Delta H° - T\Delta S° = -RTlnK \qquad (Eq.2)$$

where $R$ is the universal gas constant (8.314 J $K^{-1}$ $mol^{-1}$), $K$ corresponds to $K_A$ at specific temperatures and $T$ is the absolute temperature. The results are presented in Figure 6 and Table 1. The negative $\Delta G°$ value indicates that the binding processes of squaraine to mucin are spontaneous at the corresponding temperatures. The $\Delta H°$ and $\Delta S°$

values are both positive demonstrating that hydrophobic forces play the major role in the interaction of squaraines with PGM.

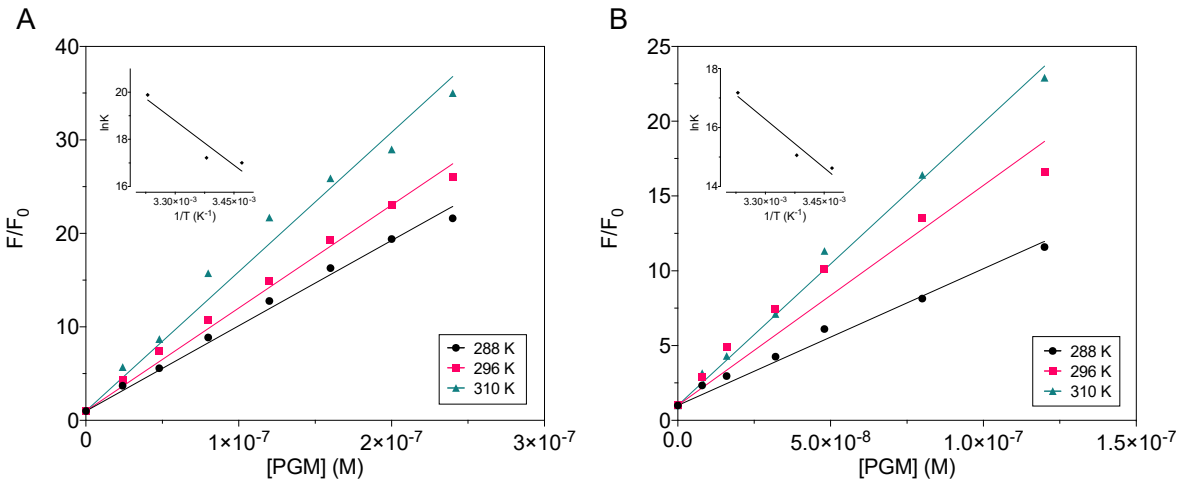


**Figure 6**. Stern-Volmer plots of S3- and S4- PGM complexes recorded at different temperatures. Van't Hoff plots are reported as insets.

**Table 1.** Thermodynamic parameters for S3- and S4-PGM complexes at various temperatures

| Compound | T (K) | $\Delta G°$(KJ mol$^{-1}$) | $\Delta H°$ (KJ mol$^{-1}$) | $\Delta S°$ (J K$^{-1}$mol$^{-1}$) |
|---|---|---|---|---|
| S3 | 288 | -40.7 | | |
| | 296 | -42.4 | 101.8 | 491.8 |
| | 310 | -51.2 | | |
| S4 | 288 | -35.0 | | |
| | 296 | -37.1 | 89.1 | 429.2 |
| | 310 | -44.3 | | |

As a result of the formation of aggregates, each squaraine exhibited very low fluorescence quantum yield in aqueous medium (QY 1-3%) however, after addition of PGM an increase of the QY was recorded (Table 2). As shown in Figure 7, the major increase in fluorescence QY was achieved by the squaraines with the longer alkyl chains. Among the four squaraines studied, S3 and S4 are the most lipophilic having logP 7.6 and 9.8 respectively (calculated with MarvinSketch, Chemaxon [41]). A high lipophilicity implies a scarce capacity to solubilize in water consequently we can assume that S3 and S4 are most prone to form aggregates in aqueous media.

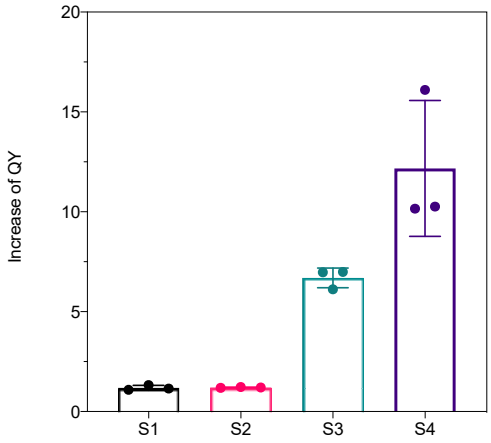


**Figure 7**. The increase of fluorescence quantum yield of squaraines in water (2% DMSO) after addition of mucin.

**Table 2**. Quantum yields ($\Phi$, expressed as percent) of the studied squaraines in water in absence and presence of PGM. Data are the mean of three measurements

| Dye | $\Phi$ | $\Phi$ (+) PGM | Increase of $\Phi$ |
|---|---|---|---|
| S1 | 3.1 | 3.6 | 1.2 |
| S2 | 3.4 | 4.1 | 1.2 |
| S3 | 1.5 | 9.8 | 6.7 |
| S4 | 0.2 | 2.8 | 12.2 |

In order to characterize possible changes in the secondary structure of mucin caused by the interaction with the squaraines, we compared the circular dichroism spectra of mucin alone and after addition of the dyes. The CD spectrum of PGM presents a maximum at 190 nm and a minimum at 208 nm (Figure 8). This is characteristic of proteins with $\alpha$-helix, $\beta$ strand and aperiodic secondary structure [42]. After addition of squaraines, it can be observed that there was a slight increase of both the band without any significant shifts. These observations imply that the interaction of squaraines with mucin causes a very small change in secondary structure of the protein.

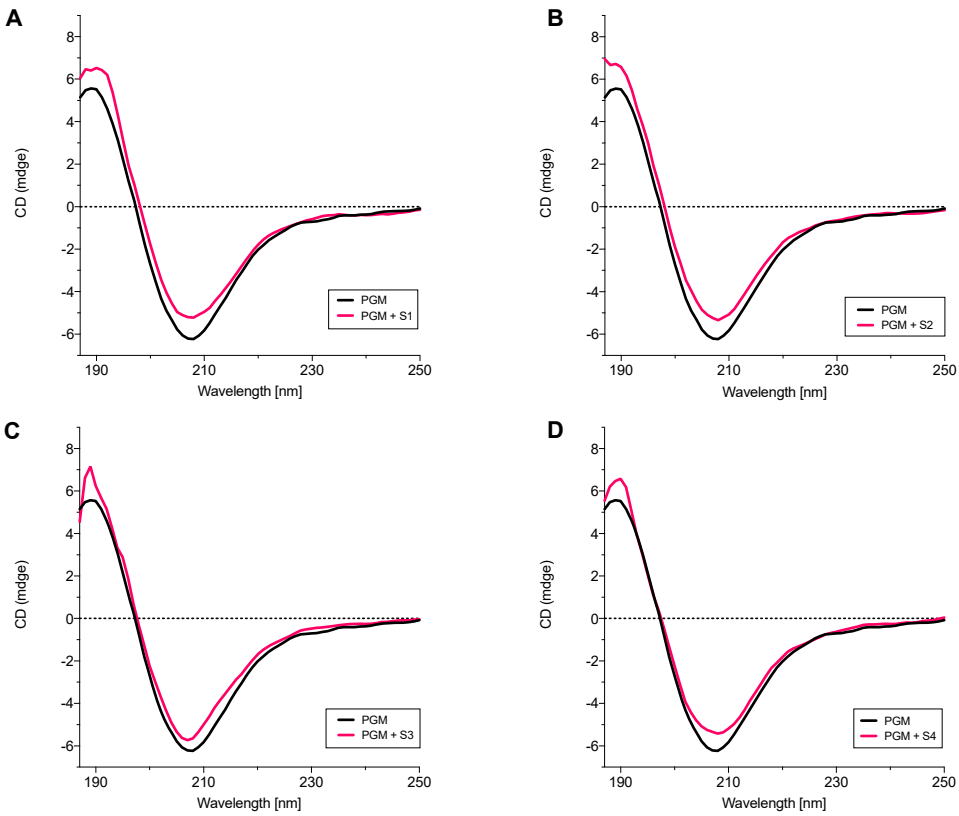


**Figure 8**. Circular dichroism spectra of mucin alone and in the presence of S1 (A), S2 (B), S3 (C) and S4 (D) recorded in water.

### 3.2. Binding and kinetic results of squaraines with PGM

Conscious of the fact that the squaraine dyes exhibit different binding and interaction kinetics based on the complexity of their molecular structure [27,43], in order to investigate the interaction between PGM and the four squaraines we performed time-resolved and kinetics fluorescent studies.

At first, binding constants were obtained by plotting the ratio of the maximum values of fluorescence intensity of the squaraine/PGM complex on the maximum of fluorescence of squaraine alone ($F/F_0$), against the increasing PGM concentration (Figure 9). Data were fitted with a non-linear least-squares procedure, based on *Eq. 3* [44].

$$\frac{F}{F_0} = \frac{F_{max}[Q]}{K_D + [Q]} \qquad (Eq. 3)$$

where $[Q]$ is the concentration of PGM, $F_{max}$ is the maximum increase of fluorescence achieved by the Sq-PGM complex formed at saturation and $K_D$ is the equilibrium dissociation constant.

In order to reduce the inner filter effect, we used concentrations of mucin lower than 1 mg/mL; however, such a concentration is not enough for S3-PGM and S4-PGM to reach a complete plateau but enough to overtake the linear range. Emission spectra were recorded after waiting for the equilibration of the squaraine-protein complexes (almost 20 min for S2- and S3-PGM complexes and 6 h for S4-PGM complex). The monomeric form of mucin weights about 640 kDa however, the extraction and purification processes alter the final protein structure [45], thus the precise value of the molecular weight is mutable. For the molecular weight of porcine gastric mucin we referred

at the work of K. Jumel et al [46]. Values of association ($K_A$) and dissociation ($K_D$) constant are reported in Table 3. We observe a dependence between the binding and the molecular structure of the squaraine. It seems like the bulkier the molecular structure of the squaraine the lowest the affinity toward mucin.

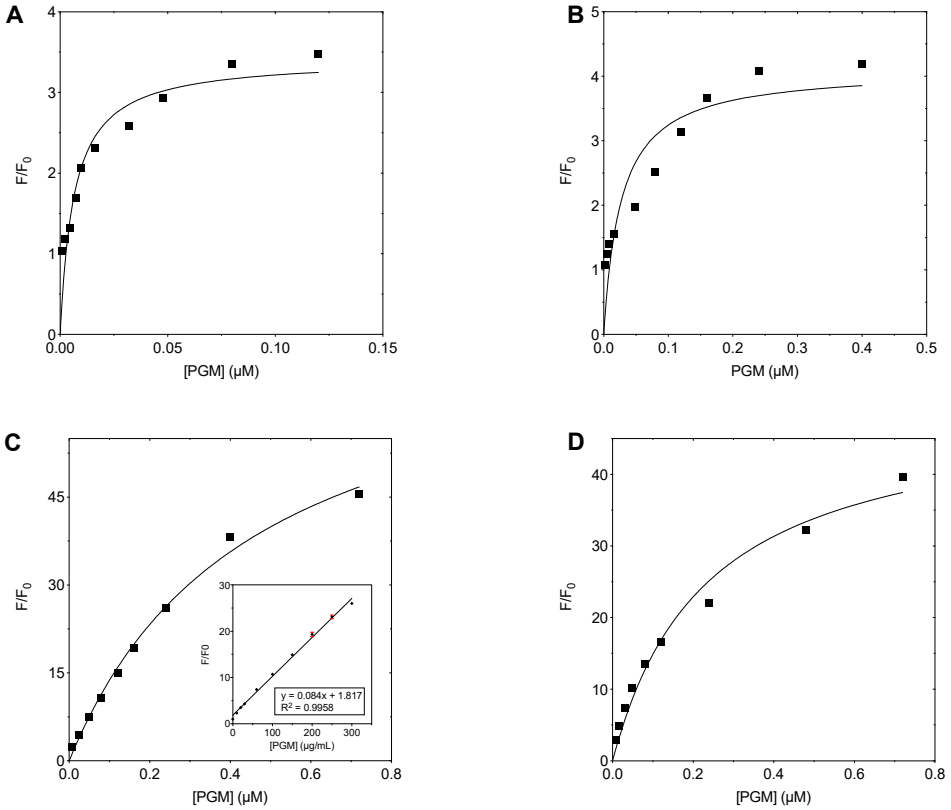


**Figure 9**. Intensity maxima obtained at various PGM concentration for the monitoring of the S1-PGM (A), S2-PGM (B), S3-PGM (C) and S4-PGM (D) complexes formation. The curve is the fitting to a hyperbole equation for the evaluation of the binding constant. Inset (in C) is the linear relationship between $F/F_0$ and [PGM] ranging from 10 to 300 µg/mL.

**Table 3**. Association ($K_A$) and dissociation ($K_D$) constants of the squaraine-PGM complexes.

| Compound | $K_A$ ($10^6$ $M^{-1}$) | $K_D$ ($10^{-7}$ M) |
|---|---|---|
| S1 | 156 (± 64) | 0.064 (± 0.026) |
| S2 | 37.2 (± 15) | 0.27 (± 0.11) |
| S3 | 2.78 (± 0.26) | 4.57 (± 0.54) |
| S4 | 4.29 (± 0.81) | 2.33 (± 0.44) |

The kinetics of the squaraine-protein complexes was then investigated by checking the variation of the emission intensity at the squaraine specific emission wavelength over time, during incubation with a constant concentration of mucin. We considered as achievement of fluorescence stability the time after which no more increase in emission intensity was observed (Figure 10). After one minute, fluorescence of S1-PGM complex was stable over time with no significant changes, while S2 and S3 required a longer time, 15 and 20 minutes respectively. Interestingly, a very long time was required for S4 which reached the plateau after 360 minutes. Based on these results, we can

assume that there is a relationship between the structure of the squaraine and the interaction with mucin, as previously found for the squaraine- bovine serum albumin interaction [27]. Evidently, the presence of short alkyl chains and indolenine groups (S1) allows a rapid kinetics. On the other hand, a slower kinetics is observed if the longer alkyl chains or the benzoindolenine groups are present (S2, S3), while the presence of both the structures on the same molecule (S4) involves a sum effect upon kinetics. It is also evident that the kinetic of the interaction has a great influence on the turn-on phenomenon: we observe a major increase of fluorescence with the long-lasting interactions (i.e. S4) while it is less evident for squaraines with fast kinetic (i.e. S1).

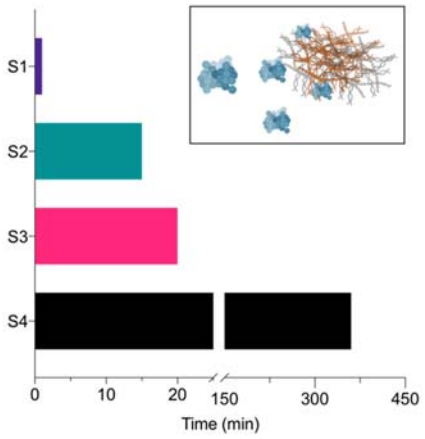


**Figure 10**. Time-dependent fluorescence intensity of squaraines in water solution in the presence of a constant concentration of mucin. The times reported are the time after which no more increase of emission was observed. Inset reports a cartoon of the interaction between squaraine aggregates and mucin.

The complex formation between the squaraines with the major increase of quantum yield (i.e. S3 and S4) and mucin was further confirmed by analysis of lifetimes. Time-resolved fluorescence analysis indicated that S3 and S4 alone exhibits a biexponential decay in water (probably due to the presence of the dye alone and dye-aggregates), whereas triexponential decay (due to the formation of dye-protein aggregates) with significantly increased lifetime was observed in presence of PGM (Figure 11).

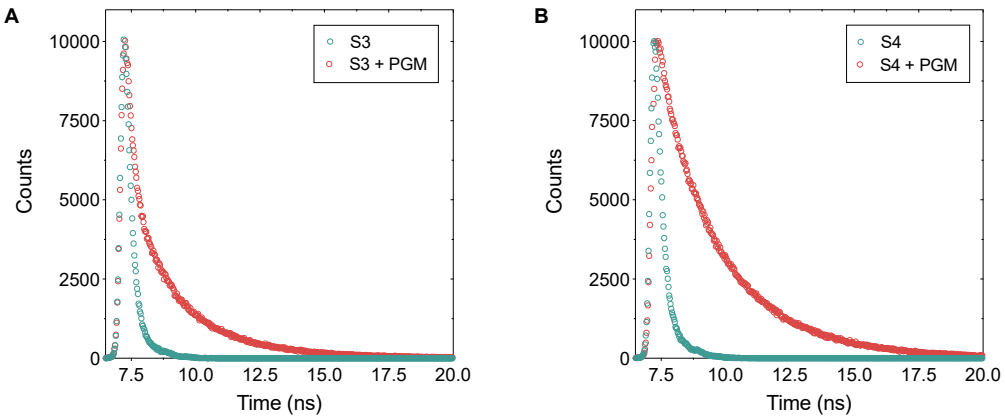


**Figure 11**. Time-resolved fluorescence analysis of S3 (A) and S4 (B) alone and in presence of PGM.

### 3.3. Detection of S3 in diluted human serum samples

As the S3-PGM complex has the major increase in fluorescence, we chose to use S3 as probe to detect mucin in serum samples. The increase of $F/F_0$ upon increasing the PGM concentration has a linear relationship in the range 10-300 µg/mL, where F represents the maximum of fluorescence intensity of the complex and $F_0$ is the maximum of fluorescence intensity of S3 alone in water. We added different concentrations of PGM into the diluted serum samples and detected it again after an equilibration period time of 30 min. The concentration of PGM in diluted serum sample was calculated using the calibration curve (Figure 9, inset in C). The calculated limit of detection (LOD) was 800 ng/mL. LOD was calculated according to the IUPAC definition of three times the deviation of the blank signal on the slope of the calibration curve ($LOD = 3\sigma\ s^{-1}$). TCA was used to remove protein from the pure serum. The procedure of detection is illustrated in Figure 12 and results are presented in Table 3: the recovery rates of different concentrations of PGM in diluted serum were from 94.9 to 116.2%. These results indicate that the squaraine S3 could act as a fluorescent probe for an accurate mucin detection in biological samples and has a great potential as an effective detection method for mucin detection in diagnostic applications.

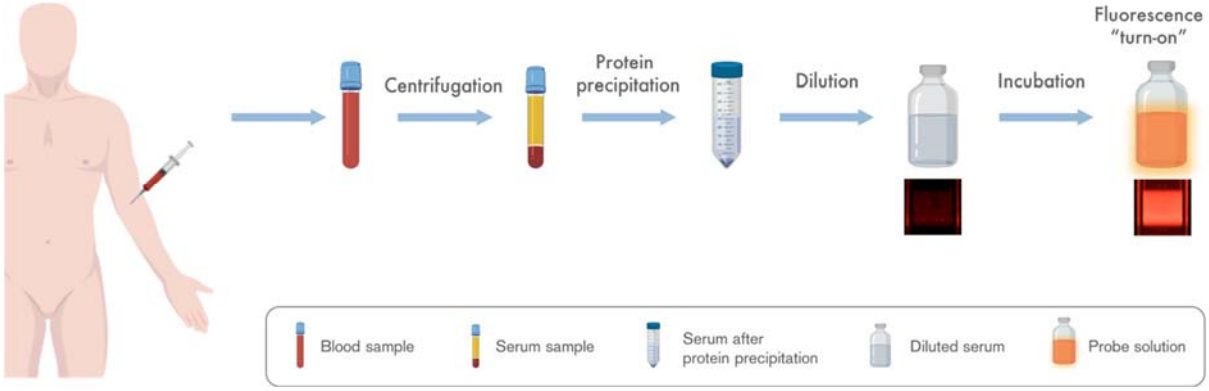


**Figure 12**. Schematic illustration of serum samples preparation and detection. The square insets want to illustrate the emission enhancement visible on the surface of the cuvette when the beam of the spectrofluorometer passes through the cuvette without and with mucin.

**Table 3**. Recovery of PGM from serum samples (n=3). Data are mean ± standard deviation (SD)

| Added PGM (µg/mL) | Detected (µg/mL) | Recovery (%) | SD (%, n=3) |
|---|---|---|---|
| 20 | 20.4 | 101.8 | 13.6 |
| 40 | 46.5 | 116.2 | 3.1 |
| 80 | 76.0 | 94.9 | 4.8 |

## 4. Conclusions

In summary, the interaction between porcine gastric mucin (PGM) and a series of squaraines with different substitutions was investigated. Thermodynamic and kinetic data were obtained. Squaraine dyes showed a structure-relationship influence upon the kinetic interaction with mucin, particularly the bulkier the molecular structure of squaraine, the slower the interaction. In addition, squaraine-mucin complexes displayed interesting emission characteristics since a fluorescence “turn-on” behavior was observed upon increasing additions of mucin

in aqueous medium with a good increase of fluorescence quantum yield. Hydrophobic interactions play an important role in the binding of squaraines with mucin. These results make the herein squaraines as potential biosensors for different biological applications. In particular, squaraine S3 showed interesting fluorescence turn-on properties for mucin detection. This novel mucin detection has several significant advantages as it is simple, robust, cost efficiency, and has an acceptable sensitivity for mucin type III. Moreover, the proposed method could be a straightforward method for *in vitro* monitoring of mucin in microscopy applications. Further studies could be conducted on this path in order to design and develop new and more efficient squaraines for the detection of biomolecules as mucins.

**Acknowledgements**

The project leading to these results has received funding from the European Union's Horizon 2020 research and innovation programme under grant agreement No 863170. All the authors acknowledge the financial support from the University of Torino (Ricerca Locale ex-60%, Bando2018).

**Conflict of interest**

The Authors declare no conflict of interest.

**Corresponding Author**

sonja.visentin@unito.it

Department of Molecular Biotechnology and Health Sciences, University of Torino, Via Gioacchino Quarello 15A, 10135 Torino (Italy)

REFERENCES

[1] J. Ma, B.K. Rubin, J.A. Voynow, Mucins, Mucus, and Goblet Cells, Chest. 154 (2017) 169–176. https://doi.org/10.1016/j.chest.2017.11.008.

[2] R. Bansil, B.S. Turner, The biology of mucus: Composition, synthesis and organization, Adv. Drug Deliv. Rev. 124 (2018) 3–15. https://doi.org/10.1016/j.addr.2017.09.023.

[3] R. Bansil, B.S. Turner, Mucin structure, aggregation, physiological functions and biomedical applications, Curr. Opin. Colloid Interface Sci. 11 (2006) 164–170. https://doi.org/10.1016/j.cocis.2005.11.001.

[4] G.C. Hansson, Mucus and mucins in diseases of the intestinal and respiratory tracts, J. Intern. Med. 285 (2019) 479–490.

[5] S.K. Behera, A.B. Praharaj, B. Dehury, Exploring the role and diversity of mucins in health and disease with special insight into non-communicable diseases, Glycoconj. J. 32 (2015) 575–613. https://doi.org/10.1007/s10719-015-9606-6.

[6] H. Suh, K. Pillai, D.L. Morris, Mucins in pancreatic cancer: biological role, implications in carcinogenesis and applications in diagnosis and therapy, Am J Cancer Res. 7 (2017) 1372–1383.

[7] N. Jonckheere, N. Skrypek, I. Van Seuningen, Mucins and Pancreatic Cancer, Cancers (Basel). 2 (2010) 1794–1812.

[8] S. Nakamori, D.M. Ota, K.R. Cleary, K. Shirotani, T. Irimura, MUC1 Mucin Expression as a Marker of Progression and Metastasis of Human Colorectal Carcinoma, Gastroenterology. 106 (1994) 353–361. https://doi.org/10.1016/0016-5085(94)90592-4.

[9] E.A. Rakha, R.W.G. Boyce, D.A. El-rehim, T. Kurien, A.R. Green, E.C. Paish, J.F.R. Robertson, I.O. Ellis, Expression of mucins (MUC1, MUC2, MUC3, MUC4, MUC5AC and MUC6) and their prognostic significance in human breast cancer, Mod. Pathol. 18 (2005) 1295–1304. https://doi.org/10.1038/modpathol.3800445.

[10] S.C. Chauhan, K. Vannatta, M.C. Ebeling, N. Vinayek, A. Watanabe, K.K. Pandey, M.C. Bell, M.D. Koch, H. Aburatani, Y. Lio, M. Jaggi, Expression and Functions of Transmembrane Mucin MUC13 in Ovarian Cancer, Cancer Res. 69 (2009) 765–775. https://doi.org/10.1158/0008-5472.CAN-08-0587.

[11] H.O. Duarte, D. Freitas, C. Gomes, J. Gomes, A. Magalhães, C.A. Reis, Mucin-Type O -Glycosylation in Gastric Carcinogenesis, Biomolecules. 6 (2016) 1–19. https://doi.org/10.3390/biom6030033.

[12] A. V Maker, N. Katabi, M. Gonen, R.P. Dematteo, M.I.D. Angelica, Y. Fong, W.R. Jarnagin, M.F. Brennan, P.J. Allen, Pancreatic Cyst Fluid and Serum Mucin Levels Predict Dysplasia in Intraductal Papillary Mucinous Neoplasms of the Pancreas, Ann. Surg. Oncol. 18 (2011) 199–206. https://doi.org/10.1245/s10434-010-1225-7.

[13] K. Chen, O. Blixt, H.H. Wandall, Mucins as biomarkers in cancer, in: Mucins and Cancer, Future Medicine Ltd, 2013: pp. 34–49. https://doi.org/10.2217/fmeb2013.13.124.

[14] J.-Y. Shih, S.-C. Yang, C.-J. Yu, H.-D. Wu, Y.-S. Liaw, R. Wu, P.-C. Yang, Elevated Serum Levels of Mucin-associated Antigen in Patients with Acute Respiratory Distress Syndrome, Am. J. Respir. Crit. Care Med. 156 (1997) 1453–1457.

[15] S. Bademler, A. Zirtiloglu, M. Sari, M.Z. Ucuncu, E.B. Dogru, S. Karabulut, Clinical Significance of Serum Membrane-Bound Mucin-2 Levels in Breast Cancer, Biomolecules. 9 (2019) 40.

[16] E. Danese, O. Ruzzenente, A. Ruzzenente, C. Iacono, Assessment of bile and serum mucin5AC in cholangiocarcinoma : Diagnostic performance and biologic significance, Surgery. 156 (n.d.) 1218–1224. https://doi.org/10.1016/j.surg.2014.05.006.

[17] M. V. Croce, M.T. Isla-Larriain, S.O. Demichelis, J.R. Gori, M.R. Price, A. Segal-Eiras, Tissue and serum MUCl mucin detection in breast cancer patients, Cancer Res. Treat. 81 (2003) 195–207.

[18] Y. Ding, J. Ling, H. Wang, J. Zou, K. Wang, X. Xiao, M. Yang, Fluorescent detection of Mucin 1 protein based on aptamer functionalized biocompatible carbon dots and graphene oxide, Anal. Methods. 7 (2015) 7792–7798. https://doi.org/10.1039/c5ay01680k.

[19] W. Wang, Y. Wang, H. Pan, S. Cheddah, C. Yan, Aptamer-based fluorometric determination for mucin 1 using gold nanoparticles and carbon dots, Microchim. Acta. 186 (2019). https://doi.org/10.1007/s00604-019-3516-4.

[20] Y. He, Y. Lin, H. Tang, D. Pang, A graphene oxide-based fluorescent aptasensor for the turn-on detection of epithelial tumor marker mucin 1, Nanoscale. 4 (2012) 2054–2059. https://doi.org/10.1039/c2nr12061e.

[21] J. Shi, Q. Deng, C. Wan, M. Zheng, F. Huang, B. Tang, Fluorometric probing of the lipase level as acute

pancreatitis biomarkers based on interfacially controlled aggregation-induced emission (AIE), Chem. Sci. 8 (2017) 6188–6195. https://doi.org/10.1039/C7SC02189E.

[22] J. Park, C. Barolo, F. Sauvage, N. Barbero, C. Benzi, P. Quagliotto, S. Coluccia, D. Di Censo, M. Grätzel, M.K. Nazeeruddin, G. Viscardi, Symmetric vs. asymmetric squaraines as photosensitisers in mesoscopic injection solar cells: A structure-property relationship study, Chem. Commun. 48 (2012) 2782–2784. https://doi.org/10.1039/c2cc17187b.

[23] L. Serpe, S. Ellena, N. Barbero, F. Foglietta, F. Prandini, M.P. Gallo, R. Levi, C. Barolo, R. Canaparo, S. Visentin, Squaraines bearing halogenated moieties as anticancer photosensitizers: Synthesis, characterization and biological evaluation, Eur. J. Med. Chem. 113 (2016) 187–197. https://doi.org/10.1016/j.ejmech.2016.02.035.

[24] M. Shimi, V. Sankar, M.K.A. Rahim, P.R. Nitha, S. Das, K. V. Radhakrishnan, K.G. Raghu, Novel glycoconjugated squaraine dyes for selective optical imaging of cancer cells, Chem. Commun. 53 (2017) 5433–5436. https://doi.org/10.1039/c6cc10282d.

[25] C.A. Bertolino, G. Caputo, C. Barolo, G. Viscardi, S. Coluccia, Novel heptamethine cyanine dyes with large stoke's shift for biological applications in the near infrared, J. Fluoresc. 16 (2006) 221–225. https://doi.org/10.1007/s10895-006-0094-8.

[26] B. Ciubini, S. Visentin, L. Serpe, R. Canaparo, A. Fin, N. Barbero, Design and synthesis of symmetrical pentamethine cyanine dyes as NIR photosensitizers for PDT, Dye. Pigment. 160 (2019) 806–813. https://doi.org/10.1016/j.dyepig.2018.09.009.

[27] N. Barbero, C. Butnarasu, S. Visentin, C. Barolo, Squaraine Dyes: Interaction with Bovine Serum Albumin to Investigate Supramolecular Adducts with Aggregation-Induced Emission (AIE) Properties, Chem. - An Asian J. 14 (2019). https://doi.org/10.1002/asia.201900055.

[28] Y. Xu, Z. Li, A. Malkovskiy, S. Sun, Y. Pang, Aggregation Control of Squaraines and Their Use as Near-Infrared Fluorescent Sensors for Protein, J. Phys. Chem. B. 114 (2010) 8574–8580.

[29] Y. Zhang, X. Yue, B. Kim, S. Yao, M. V Bondar, K.D. Belfield, Bovine Serum Albumin Nanoparticles with Fluorogenic Near-IR-Emitting Squaraine Dyes, ACS Appl. Mater. Interfaces. 5 (2013) 8710–8717. https://doi.org/10.1021/am402361w.

[30] V.S. Jisha, K.T. Arun, M. Hariharan, D. Ramaiah, Site-Selective Binding and Dual Mode Recognition of Serum Albumin by a Squaraine Dye, J. AM. CHEM. SOC. 128 (2006) 6024–6025. https://doi.org/10.1021/ja061301x.

[31] V.S. Jisha, K.T. Arun, M. Hariharan, D. Ramaiah, Site-Selective Interactions- Squaraine Dye-Serum Albumin Complexes with Enhanced Fluorescence and Triplet Yields, J. Phys. Chem. B. 114 (2010) 5912–5919.

[32] C. Butnarasu, N. Barbero, D. Pacheco, P. Petrini, S. Visentin, Mucin binding to therapeutic molecules : The case of antimicrobial agents used in cystic fi brosis, Int. J. Pharm. 564 (2019) 136–144. https://doi.org/10.1016/j.ijpharm.2019.04.032.

[33] N. Barbero, C. Magistris, J. Park, D. Saccone, P. Quagliotto, R. Buscaino, C. Medana, C. Barolo, G. Viscardi, Microwave-Assisted Synthesis of Near-Infrared Fluorescent Indole-Based Squaraines, Org. Lett. 17 (2015) 3306–3309. https://doi.org/10.1021/acs.orglett.5b01453.

[34] J. Park, N. Barbero, J. Yoon, E. Dell'Orto, S. Galliano, R. Borrelli, J.H. Yum, D. Di Censo, M. Grätzel, M.K. Nazeeruddin, C. Barolo, G. Viscardi, Panchromatic symmetrical squaraines: A step forward in the molecular engineering of low cost blue-greenish sensitizers for dye-sensitized solar cells, Phys. Chem. Chem. Phys. 16 (2014) 24173–24177. https://doi.org/10.1039/c4cp04345f.

[35] F. Gao, Y. Lin, L. Li, Y. Liu, U. Mayerhöffer, P. Spenst, J. Su, J. Li, F. Würthner, H. Wang, Supramolecular adducts of squaraine and protein for noninvasive tumor imaging and photothermal therapy in vivo, Biomaterials. 35 (2014) 1004–1014. https://doi.org/10.1016/j.biomaterials.2013.10.039.

[36] Y. Xu, Q. Liu, X. Li, Y. Pang, A zwitterionic squaraine dye with a large Stokes shift for in vivo and site-selective protein sensing w, Chem. Commun. (2012) 11313–11315. https://doi.org/10.1039/c2cc36285f.

[37] F. An, Z. Deng, J. Ye, J. Zhang, Y. Yang, C. Li, C. Zheng, X. Zhang, Aggregation-Induced Near-Infrared Absorption of Squaraine Dye in an Albumin Nanocomplex for Photoacoustic Tomography in Vivo, Appl. Mater. Interfaces. 6 (2014) 17985–17992.

[38] G.M. Paternò, L. Moretti, A.J. Barker, C. D'Andrea, A. Luzio, N. Barbero, S. Galliano, C. Barolo, G. Lanzani, F. Scotognella, Near-infrared emitting single squaraine dye aggregates with large Stokes shifts, J. Mater. Chem. C. 5 (2017) 7732–7738. https://doi.org/10.1039/c7tc01375b.

[39] G. Wang, W. Xu, Y. Guo, N. Fu, Near-infrared squaraine dye as a selective protein sensor based on self-assembly, Sensors Actuators B. Chem. 245 (2017) 932–937. https://doi.org/10.1016/j.snb.2017.01.172.

[40] J. Caicedo, E.J. Perilla, Effect of pH on the rheological response of reconstituted gastric mucin, Ing. e Investig. 35 (2015) 43–48.

[41] MarvinSketch 18.28, ChemAxon, (n.d.).

[42] A. Jabrani, S. Makamte, E. Moreau, Y. Gharbi, A. Plessis, M. Sanial, V. Biou, Biophysical characterisation of the novel zinc binding property in Suppressor of Fused, Sci. Rep. 7 (2017) 2–11. https://doi.org/10.1038/s41598-017-11203-2.

[43] N. Barbero, S. Visentin, G. Viscardi, The different kinetic behavior of two potential photosensitizers for PDT, J. Photochem. Photobiol. A Chem. 299 (2015) 38–43. https://doi.org/10.1016/j.jphotochem.2014.11.002.

[44] C. Pontremoli, N. Barbero, G. Viscardi, S. Visentin, Mucin-drugs interaction: The case of theophylline, prednisolone and cephalexin, Bioorganic Med. Chem. 23 (2015) 6581–6586. https://doi.org/10.1016/j.bmc.2015.09.021.

[45] K. Bidmon, O. Lieleg, S. Berensmeier, An optimized purification process for porcine gastric mucin with preservation of its native functional properties, RSC Adv. 6 (2016) 44932–44943. https://doi.org/10.1039/C6RA07424C.

[46] K. Jumel, I. Fiebrig, S.H. E., Rapid size distribution and purity analysis of gastric mucus glycoproteins by size exclusion chromatography: multi angle laser light scattering, Biol. Macromol. 18 (1996) 133–139.